ACS Photonics

Letter

pubs.acs.org/journal/apchd5

Chemically Tunable, Biocompatible, and Cost-Effective Metal–Insulator–Metal Resonators Using Silk Protein and Ultrathin Silver Films

Hyunsoo Kwon[†] and Sunghwan Kim[*,†,‡]

[†]Department of Energy Systems Research and [‡]Department of Physics, Ajou University, Suwon 16499, Republic of Korea

Supporting Information

ABSTRACT: Responsive optical resonators are used in chemical and biological sensing applications because their optical properties can be tuned by interactions with their environment. The use of non-nanostructured designs and biological materials expands the applications of these resonators because of their biocompatibility and low cost. Natural silk protein enables designing cost-effective, biocompatible, and chemically tunable metal–insulator–metal (MIM) resonators for color filters and superabsorbers. Our resonant silk MIM exhibited a red shift of the resonance through swelling, which could be controlled by stimuli such as pH and alcohol concentration. The absorption could be detected even in highly scattering biological tissues. Additionally, deep UV light was applied to generate arbitrary patterns with a different color than the background. The proposed silk MIM resonator, which was tunable, biocompatible, and cost-effective, would be useful as a spectral signature in chemical and biological sensing applications.

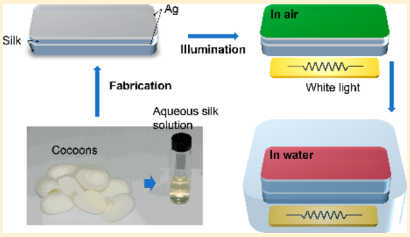

KEYWORDS: *metal–insulator–metal resonator, silk protein, chemically tunable, color filter, superabsorber*

Planar and multilayered optical devices recently resurfaced as alternative candidates in controlling and manipulating light–matter interactions with the advantage of unprecedented performance and cost-effective fabrication.[1−6] Specifically, planar and lithography-free metal–insulator–metal (MIM) resonators based on a Fabry–Perot etalon exhibit highly efficient spectral windows and omnidirectional properties;[4−6] therefore, these optical properties can be useful in chemical and biological sensing applications when used in conjunction with flexible platforms. However, conventional planar MIM resonators lack sensing capability because it is difficult for analytes to exert influence on the physical variables of the insulating layer in which optical fields are strongly localized.

Silk fibroin, the natural protein extracted from the *Bombyx mori* caterpillar, is an attractive material in nano- and bio-optics because of its optical transparency, biocompatibility, and robust mechanical properties.[7,8] Various silk-based optical devices have been demonstrated, including photonic crystals,[9] waveguides,[10] and single-mode lasers.[11] In particular, the favorable combination of noble metals and silk leads to a fully biocompatible and free-standing optical device that can be implanted in living tissue with no immune response.[12−14] Crystallized silk film with hydrogel properties serves as a molecular network with nanochannels for analytes to penetrate and therefore can induce drastic changes in the optical resonances due to swelling.[14] These properties of silk protein can provide a solution to overcome the lack of sensing capability of conventional MIM resonators.

Here we report chemically tunable, biocompatible, and cost-effective MIM resonators that can be color filters and superabsorbers. Silk films were used as the substrate and ultrathin insulator layer, which was sandwiched between two ultrathin silver (Ag) layers to yield a free-standing and flexible MIM resonator. By taking advantage of the hydrogel properties of silk, the resonance wavelengths could be tuned via swelling of the silk insulator layer, which was caused by chemical interactions with the environment, such as the alcohol concentration and pH. This responsive silk MIM resonator had an extremely large optical tunability wavelength range due to changes in both the layer thickness and refractive index (RI). Deep UV light was used to generate arbitrary patterns with different colors, which might be useful as color codes for sensors. Additionally, we could detect the resonance of a MIM resonator buried conformingly beneath chicken breast tissue, and we confirmed that the reflected signal was more easily detected in the near-infrared window of tissue. These properties could provide opportunities for application to human-implantable, biocompatible, biodegradable, highly efficient biochemical sensors.

RESULTS AND DISCUSSION

A schematic diagram and the operating principle of the proposed silk MIM resonator are shown in Figure 1a. The transmission-type color filter consists of a metallic resonator that incorporates an insulating silk film sandwiched between two ultrathin Ag films. This resonator mimics a MIM Fabry–Perot etalon and is basically considered a bandpass filter. The core element of the device is the silk insulating layer. A simple

Received: August 21, 2015
Published: November 16, 2015

DOI: 10.1021/acsphotonics.5b00470
ACS Photonics 2015, 2, 1675−1680

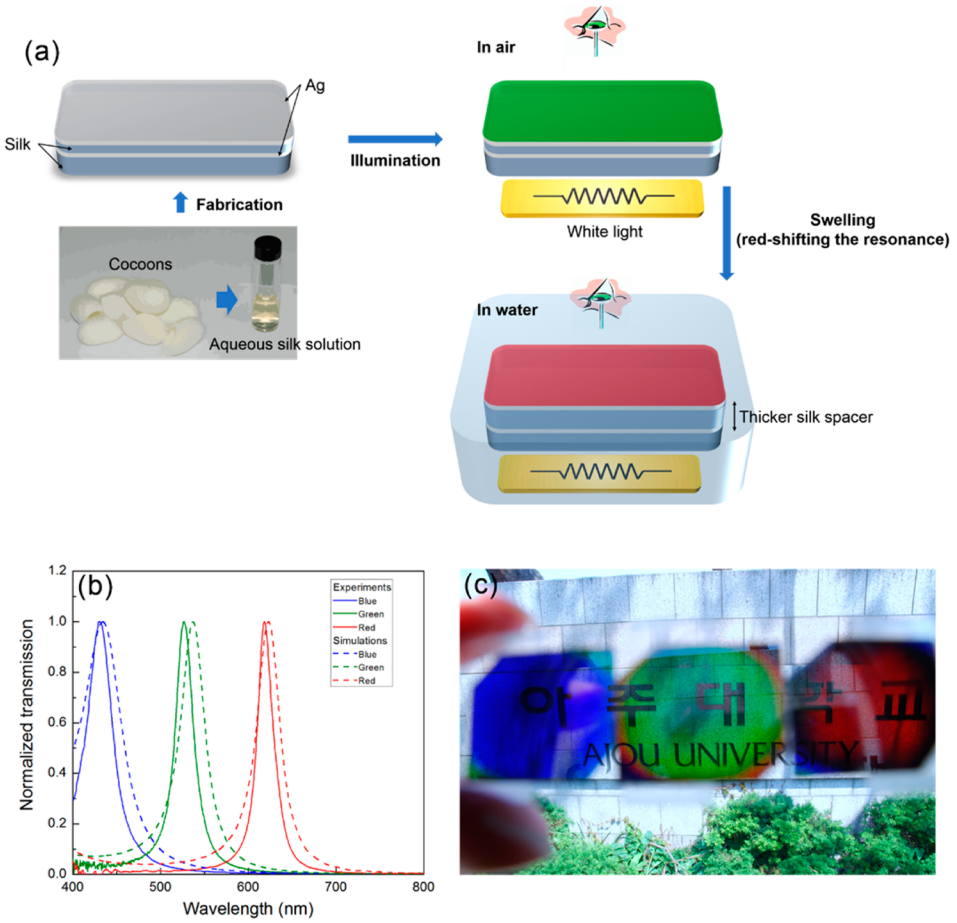

Figure 1. Proposed silk metal−insulator−metal (MIM) color filters. (a) Schematic configurations to demonstrate the working principle of the planar silk MIM. Two silver (Ag) layers surround a silk spacer. The silk spacer absorbs the liquid in the environment, which induces swelling. The changes in the volume and refractive index of the swollen silk layer result in drastic changes in the resonance modes. (b) Measured and simulated transmission spectra for the silk MIM color filters with silk spacer thicknesses of 90, 120, and 150 nm. (c) Photograph taken through the RGB filters used in (b).

methanol or water vapor treatment can induce β-sheet crystallization by causing hydrogen bonds to form between silk molecules, thereby making the silk layer a hydrogel.[15] The physical volume and RI of the silk insulating nanogap of the MIM resonator change when it is swollen, which induces drastic changes in the resonance modes.[14]

For the design of color filters, we performed finite-difference time domain (FDTD) simulations (see Methods). The thickness of the silk film was controlled to position the transmission peaks within the visible region, and 90, 120, and 150 nm were selected to produce blue (B), green (G), and red (R) color filters, respectively. The thicknesses of the top and bottom Ag films were chosen to be 35 nm after FDTD simulations to optimize the trade-off between the transmission and the quality factor (Q factor), which is defined as $Q = \lambda_{peak}/\Delta\lambda$, where λ_{peak} is the resonant wavelength and $\Delta\lambda$ is the full-width at half-maximum (fwhm) of the resonance (see Figure 1S in the Supporting Information). Increasing the thickness of the Ag layer results in a higher Q factor, whereas the transmission through the resonator is significantly reduced because of the higher reflection from the outer Ag−dielectric interface. The determination of the optimized thickness depended on the color of the filter, but our general design criteria for the color filter were a Q factor of 10, a maximum transmission of 50%, so that the filter could be considered transparent, and no overlap between two individual color spectra.

Consequently, as described in Figure 2S and the Methods section, our silk MIM resonators were fabricated with two 35 nm thick Ag layers using the electron beam deposition method. The thickness of the silk insulating layer was controlled via the spin-coating speed and the concentration of the silk aqueous solution. Then, we crystallized the silk insulating layer via a methanol treatment. Postcasting of the silk solution for film formation on the fabricated MIM resonator yielded a flexible, biocompatible, and free-standing MIM resonator. It is noteworthy that a free-standing silk film has a relatively higher elastic modulus than a conventional PDMS film and therefore has better resistance to deformation.[16] The flatness of the silk film was stably preserved when we took an edge of the film (see Figure 3S in the Supporting Information). This indicates that reliable optical responses can be obtained with no use of a rigid substrate. Figure 1b shows the measured and simulated transmission spectra of three silk MIMs with varying silk thicknesses. The small discrepancy between the measured and simulated spectra resulted from fabrication tolerances. A vivid and bright image taken using the fabricated RGB color filters is shown in Figure 1c.

The most notable feature of the silk MIMs is the variation in the resonances due to interaction with the environment. As a

DOI: 10.1021/acsphotonics.5b00470
ACS Photonics 2015, 2, 1675−1680

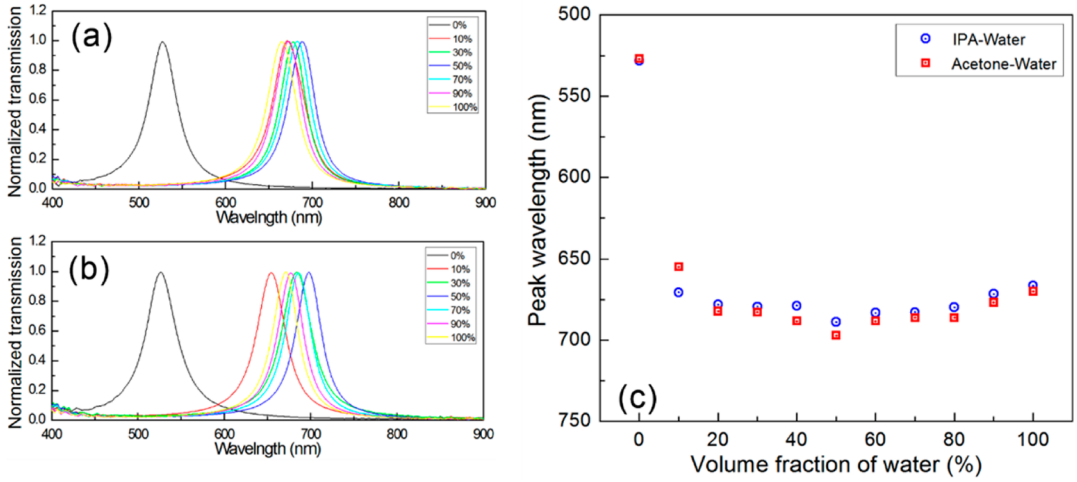

Figure 2. Resonance behavior of the silk MIM for IPA–water and acetone–water mixtures. Normalized transmission spectra for silk MIMs immersed in (a) IPA–water mixtures and (b) acetone–water mixtures (b) with varying concentrations. (c) Plot of the wavelength of the transmission peaks as a function of the concentration of water.

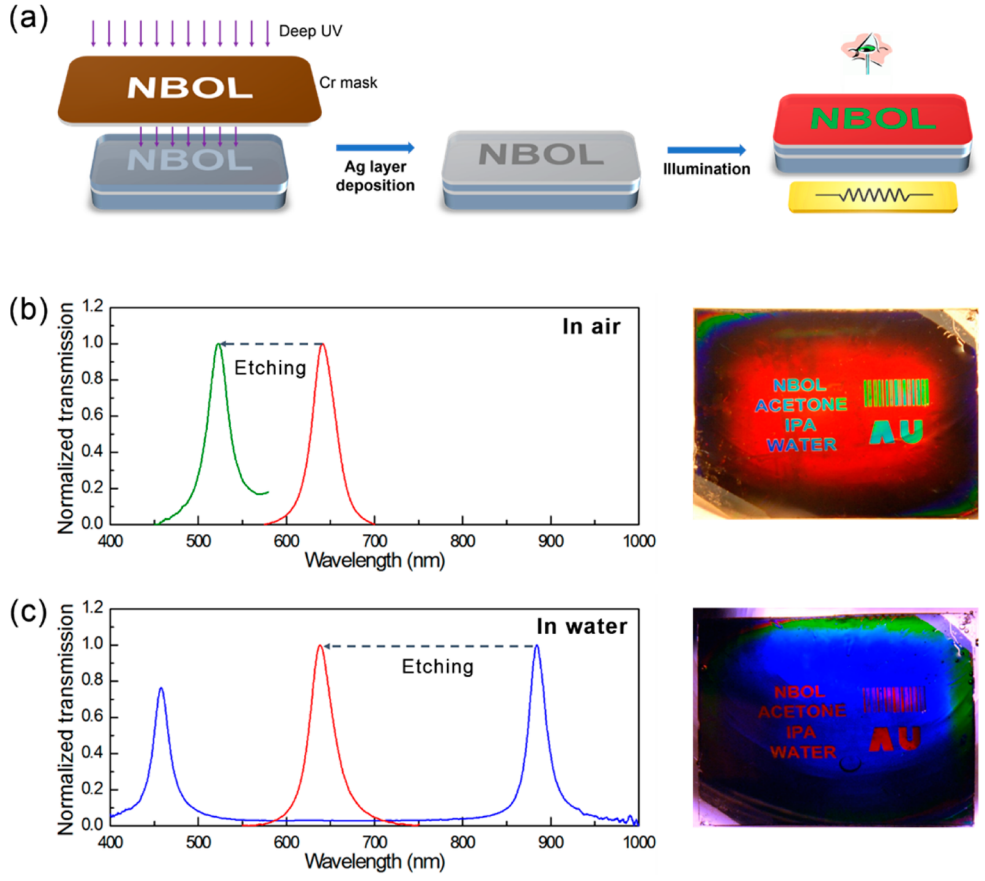

Figure 3. Color filter with two colors. (a) Schematic diagram for the fabrication using deep UV light. (b, c) Normalized transmission spectra and the corresponding photograph of the fabricated color filter in (b) air and (c) water.

proof-of-principle experiment, we measured the transmission spectra in isopropyl alcohol (IPA)–water and acetone–water mixtures with varying compositions and therefore different swelling ratios (Figure 2). The transmission peaks underwent a red shift with increasing concentration of water because of the expanded silk layer. Because the physical volume of the silk spacer where photons were strongly localized changed, we achieved red shifts of ~150 nm, which was not expected from the RI change. (For the effect of swelling on resonance, see Figure 4S in the Supporting Information.) Even though the absorbed liquid influences the RI and the volume of silk hydrogel simultaneously, simulations (Figure 4S) and our previous study[14] prove that the volume change is the prominent quantity for tuning the resonance behaviors. Figure 2c shows the variation in the spectral position of the transmission peak versus the volume fraction of water. Even a

DOI: 10.1021/acsphotonics.5b00470
ACS Photonics 2015, 2, 1675–1680

small concentration of water in mixtures could induce a huge red shift, and the swelling of the silk spacer in the 50:50 mixture was slightly larger than that of the spacer in pure water. As described in our previous study, a 50:50 mixture of solvents with weak (IPA and acetone) and strong (water) polarity can induce a larger volume expansion relative to that of the pure solvent with strong polarity; this is because organic solvent molecules can form hydrogen bonds with water molecules and then induce a reentrant transition in the silk hydrogel film.[14] This extra expansion is inversely proportional to the polarities of the organic solvents, and thus the acetone–water mixture led to a greater expansion than the IPA–water mixture.

To investigate potential applications, we generated two color patterns by direct etching of the silk spacer using deep UV light (Figure 3a). The spin-coated silk layer was first crystallized using methanol. Then, deep UV light from an ozone lamp illuminated the silk layer through the patterned chrome mask. As shown in Figure 3b, the etched letters were green in color, corresponding to a shorter resonance wavelength (λ = 523 nm) than that (λ = 640 nm) of the red background region. When immersed in water, the filtered colors were red-shifted because of swelling. A notable feature is the blue color of the unetched background region, in which the near-infrared (not visible) transmission peak was predicted. The measured spectra prove that this effect originated from the next higher order mode. One could potentially miniaturize the generated color patterns to the micro- or nanoscale using ArF excimer photolithography on silk films, as we recently reported.[17] This technology could lead to the use of our color filters in biosensor platforms with color codes, visual arts, and wearable displays.[18,19]

As an alternative application, highly absorbing resonators were investigated by making the bottom Ag layer optically thick (~200 nm) in order to eliminate light transmission. This scheme allows for the detection of absorption features in reflectance measurements. The thickness of the top Ag layer was set to 30 nm to balance strong localization and coupling of the incident light to the resonators. We designed the absorbers to have strong absorptions in the green, red, and near-infrared regions (corresponding to thicknesses of 130, 160, and 190 nm, respectively) since implantation of the resonators in biological tissues was considered. Figure 4a shows measured and simulated reflectance spectra. Because there was no transmitted light because of the optically thick bottom Ag layer, the dips in reflection exactly corresponded to the absorption peaks. The small discrepancy between the measured and simulated spectra also resulted from fabrication tolerances. Photographic images of the fabricated silk MIM resonator illuminated by indoor light are shown in Figure 4b–d. One can see three primary subtractive colors of magenta, cyan, and weak yellow for d = 130, 160, and 190 nm, respectively. These subtractive colors, which have additive counterparts of red (cyan), green (magenta), and blue (yellow), demonstrate the absorption features of the fabricated silk MIM resonators well.[20]

A possible application of silk-protein-based optical elements is to use them within biological tissues to provide non-endogenous spectral signatures because silk is biocompatible, degradable, and implantable.[9] The detectability of the spectral signatures in highly scattering tissues was validated by performing an *in vitro* experiment in which a silk MIM resonator was placed under slices of chicken breast tissue of variable thickness (Figure 5a–c). In order to detect the signatures, the incident signal must overcome scattering twice: once when reaching the MIM (after incidence) and then when

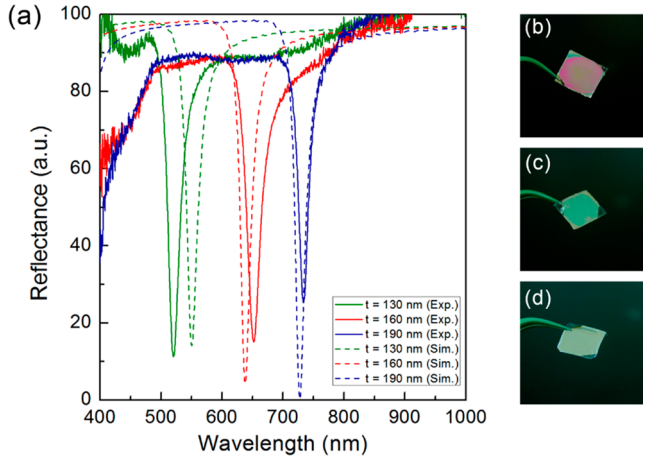

Figure 4. Silk MIM absorber. The bottom silver layer becomes optically thick (t = 200 nm) to minimize light transmission. (a) Measured (solid line) and simulated (dashed line) reflectance spectra of the silk MIM absorber with d = 130, 160, and 190 nm. (b–d) Photographs of the silk MIM absorbers illuminated by indoor light.

reaching the optical fiber (after reflection). The first optical window in biological tissues, which exists at wavelengths between 700 and 900 nm, is useful in this case for low absorption and scattering.[21] As shown in Figure 5b,c, the 830 nm reflectance dip could be detected even under 1.95 mm thick tissue, while the 620 nm reflection dip disappeared. Additionally, the pH sensitivity of a silk MIM color filter was examined by immersing it in buffer solutions with different pH values. As the pH increased, the transmission peak red-shifted (Figure 5d). We obtained a pH sensitivity of 4.15 nm per 1 pH unit change.

CONCLUSION

In conclusion, we proposed and demonstrated chemically tunable color filters and superabsorbers in the visible and near-infrared wavelength regions. A modified Fabry–Perot etalon was demonstrated using large-area, lithography-free, and cost-effective planar MIM coatings of silk fibroin and Ag. The performance, represented by the transmission, absorption, and Q factor, was comparable with that of nanostructured plasmonic devices. Swelling of the silk spacer led to the high tunability of the Fabry–Perot resonances, and this swelling ratio could be controlled by stimuli such as alcohol concentration and pH. Patterned letters of a color different than the background were achieved using simple deep UV etching. The absorptive features could be detected through 1.95 mm thick biological tissue in the near-infrared optical window of tissues. This silk MIM resonator can lead to new possibilities at the interface between nano-optics and biological applications by exploiting the favorable material properties of silk fibroin, including facile fabrication, tunability, and biocompatibility. Such a silk resonator can be used for real-time, extremely sensitive, and *in vivo* monitoring of analytes in body fluid.

METHODS

Preparation of Silk Aqueous Solution. Cocoons of *Bombyx mori* caterpillars were boiled for 60 min in a solution of 0.02 M Na_2CO_3 to remove the sericin protein. The extracted fibroin was rinsed with distilled water and then dried in air for 24 h. After drying, the fibroin was dissolved in a 9.3 M LiBr solution at 60 °C for 4 h, yielding a 20 wt % aqueous solution.

DOI: 10.1021/acsphotonics.5b00470
ACS Photonics 2015, 2, 1675–1680

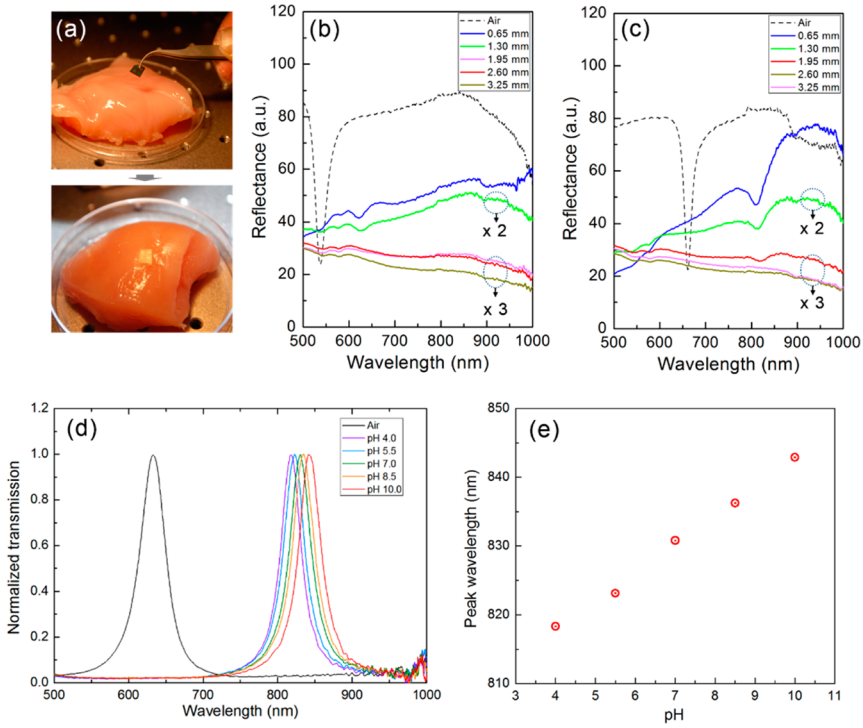

Figure 5. Optical response at the interface of the silk MIM and biological materials. (a) Conceptual images for the implantion of silk MIM resonators. (b, c) Measured spectra for the silk MIM with d = 160 nm in (b) and d = 190 nm in (c) when placed under chicken breast tissues of different thicknesses. Because of swelling, the resonance modes are red-shifted in both cases. These results prove that the spectral signature can be more easily detected in the first near-infrared window of tissue. (d) pH sensitivity of the silk MIM showing normalized transmission spectra for different pH values (pH = 4.0, 5.5, 7.0, 8.5, and 10.0). (e) Plot of the wavelength of the transmission peaks as a function of the pH value.

The silk/LiBr solution was dialyzed against distilled water using a dialysis cassette (Slide-a-Lyzwe, Pierce, MWCO 3.5 K) at room temperature for 2 days until the solution reached a concentration of 6%. The obtained solution was purified using a centrifuge and a syringe filter with a 0.45 μm pore size.

Fabrication Process. The silk MIM resonators were first generated on a silicon substrate coated with a sacrificial poly(methyl methacrylate) (PMMA) layer. The top Ag layer was deposited on the PMMA layer on the silicon substrate using an electron gun evaporator (SEE-7, ULTECH). A thin silk spacer was then formed by spin-coating a silk solution. The thickness of the silk spacer could be controlled via the spin-coating speed and the concentration of the silk solution. For a 120 nm thick silk film, the speed and concentration were 3800 rpm and 5.77%, respectively. To form a silk spacer with hydrogel properties, the sample was immersed in methanol for 1 min. The bottom Ag layer was deposited on the hydrogel silk spacer using the same evaporation method. To yield the MIM on a soft silk substrate as a free-standing form, the aqueous silk solution was cast onto the fabricated MIM resonator for a day. By dissolving the PMMA sacrificial layer in acetone, we could obtain a free-standing silk MIM resonator. The two-color MIM resonator was fabricated using deep UV etching. Deep UV light (G36T5VH, Philips) at wavelengths of 185 and 254 nm was illuminated on the silk spacer through the patterned chrome mask for 20 min. Subsequent processes after the UV exposure were the same as those for the single-color MIM resonator.

Optical Measurement. For reflection measurements, we utilized a butt-end fiber-coupling scheme. The multimode fiber end of a 1 × 2 fiber coupler with a 200 μm core diameter was butt joined to a silk MIM in the vertical direction. Optical excitation and the collection of the reflected signal could be accomplished simultaneously. The fiber-coupled white light source (LS-1, Ocean Optics) was fed through the input port, while the reflected signal from the output port was measured using an optical spectrum analyzer (USB-2000, Ocean Optics). The remaining single port end of the coupler was brought in close proximity to the silk MIM. For transmission measurements, white light was illuminated on the side of the Ag/substrate interface. The transmitted signal was coupled to a fiber tip on the opposite side and sent to the spectrometer. The reference signal was collected using an aluminum mirror.

Simulation. Numerical simulations were performed with a commercial FDTD software package (FDTD Solutions, Lumerical Solutions) to generate the reflectance and transmittance spectra. The simulation layout included perfect matching layers (PMLs) on the top and bottom boundaries of the simulation unit cell, and we used periodic boundary conditions along the lateral directions. The complex dielectric constants of silver were taken from the data in the Palik handbook. The refractive index of silk used herein was 1.54 in the visible and near-infrared range. A plane wave source, normally launched to the top of the MIM resonator, was used for structure excitation. The plane wave covered a wavelength range of 300−1000 nm with 2000 frequency points. Reflected light was recorded on the top (reflection) and the bottom (transmission) PML. The mesh size for the metal structure was 0.5 nm in the z direction and 2 nm in the x and y directions.

■ ASSOCIATED CONTENT

Supporting Information

The Supporting Information is available free of charge on the ACS Publications website at DOI: 10.1021/acsphotonics.5b00470.

DOI: 10.1021/acsphotonics.5b00470
ACS Photonics 2015, 2, 1675−1680

(S1) FDTD simulation for the optimized thickness of the top Ag layer; (S2) fabrication process; (S3) photographs showing the flexibility and the stiffness of the free-standing MIM resonator; (S4) FDTD simulation for the effect of physical variables on the resonance (PDF)

AUTHOR INFORMATION

Corresponding Author

*E-mail: sunghwankim@ajou.ac.kr.

Notes

The authors declare no competing financial interest.

ACKNOWLEDGMENTS

The authors acknowledge support from the Basic Science Program (NRF-2014R1A1A1008080), the Framework of International Cooperation Program (NRF-2014K2A1B8048519), and the Nano-Material Technology Development Program (2009-0082580) through the National Research Foundation (NRF). S.K. is also supported by the TJ Park Science Fellowship of the POSCO TJ Park Foundation.

REFERENCES

(1) Kats, M. A.; Blanchard, R.; Genevet, P.; Capasso, F. Nanometre optical coatings based on strong interference effects in highly absorbing media. *Nat. Mater.* **2013**, *12*, 20−24.

(2) Valagiannopoulos, C. A.; Tukiainen, A.; Aho, T.; Niemi, T.; Guina, M.; Trekyakov, S. A.; Simovski, C. R. Perfect magnetic mirror and simple perfect absorber in the visible spectrum. *Phys. Rev. B: Condens. Matter Mater. Phys.* **2015**, *91*, 115305.

(3) Lee, J.-H.; Koh, C. Y.; Singer, J. P.; Jeon, S.-J.; Maldovan, M.; Stein, O.; Thomas, E. L. Ordered Polymer Structures for the Engineering of Photons and Phonons. *Adv. Mater.* **2014**, *26*, 532−569.

(4) Li, Z.; Butun, S.; Aydin, K. Large-Area, Lithography-Free Super Absorbers and Color Filters at Visible Frequencies Using Ultrathin Metallic Films. *ACS Photonics* **2015**, *2*, 183−188.

(5) Lee, K.-T.; Seo, S.; Guo, L. J. High-Color-Purity Subtractive Color Filters with a Wide Viewing Angle Based on Plasmonic Perfect Absorbers. *Adv. Opt. Mater.* **2015**, *3*, 347−352.

(6) Yan, M. Metal-insulator-metal light absorber: a continuous structure. *J. Opt.* **2013**, *15*, 025006.

(7) Omenetto, F. G.; Kaplan, D. L. A new route for silk. *Nat. Photonics* **2008**, *2*, 641−643.

(8) Omenetto, F. G.; Kaplan, D. L. New Opportunities for an Ancient Material. *Science* **2010**, *329*, 528−531.

(9) Kim, S.; Mitropoulos, A. N.; Spitzberg, J. D.; Tao, H.; Kaplan, D. L.; Omenetto, F. G. Silk inverse opals. *Nat. Photonics* **2012**, *6*, 818−823.

(10) Parker, S. T.; Domachuk, P.; Amsden, J.; Bressner, J.; Lewis, J. A.; Kaplan, D. L.; Omenetto, F. G. Biocompatible Silk Printed Optical Waveguides. *Adv. Mater.* **2009**, *21*, 1−5.

(11) Choi, Y.; Jeon, H.; Kim, S. A fully biocompatible single-mode distributed feedback laser. *Lab Chip* **2015**, *15*, 642−645.

(12) Park, J.; Choi, Y.; Lee, M.; Jeon, H.; Kim, S. Novel and simple route to fabricate fully biocompatible plasmonic mushroom arrays adhered on silk biopolymer. *Nanoscale* **2015**, *7*, 426−431.

(13) Kim, S.; Mitropoulos, A. N.; Spitzberg, J. D.; Kaplan, D. L.; Omenetto, F. G. Silk protein based hybrid photonic-plasmonic crystal. *Opt. Express* **2013**, *21*, 8897−8903.

(14) Lee, M.; Jeon, H.; Kim, S. A Highly Tunable and Fully Biocompatible Silk Nanoplasmonic Optical Sensor. *Nano Lett.* **2015**, *15*, 3358−3363.

(15) Hu, X.; Kaplan, D.; Cebe, P. Determining Beta-Sheet Crystallinity in Fibrous Proteins by Thermal Analysis and Infrared Spectroscopy. *Macromolecules* **2006**, *39*, 6161−6170.

(16) Jiang, C.; Wang, X.; Gunawidjaja, R.; Lin, Y.-H.; Gupta, M. K.; Kaplan, D. L.; Naik, R. R.; Tsukruk, V. V. Mechanical Properties of Robust Ultrathin Silk Fibroin Films. *Adv. Funct. Mater.* **2007**, *17*, 2229−2237.

(17) Kim, S. Silk fibroin: a new resist for eco-friendly photolithography. *Proceeding of the Photonics West 2014*; San Francisco, CA, USA, February 1−6, 2012.

(18) Tan, S. J.; Zhang, L.; Zhu, D.; Goh, X. M.; Wang, Y. M.; Kumar, K.; Qiu, C.-W.; Yang, J. K. Plasmonic Color Palettes for Photorealistic Printing with Aluminum Nanostructures. *Nano Lett.* **2014**, *14*, 4023−4029.

(19) Nam, J.-M.; Jang, K.-J.; Groves, J. T. Detection of proteins using a colorimetric bio-barcode assay. *Nat. Protoc.* **2007**, *2*, 1438−2007.

(20) Shrestha, V. R.; Lee, S.-S.; Kim, E.-S.; Choi, D.-Y Aluminum Plasmonics Based Highly Transmissive Polarization-Independent Subtractive Color Filters Exploiting a Nanopatch Array. *Nano Lett.* **2014**, *14*, 6672−6678.

(21) Smith, A. M.; Mancini, M. C.; Nie, S. Bioimaging: Second window for *in vivo* imaging. *Nat. Nanotechnol.* **2009**, *4*, 710−711.

DOI: 10.1021/acsphotonics.5b00470
ACS Photonics 2015, 2, 1675−1680